Talanta 80 (2009) 403–406

Contents lists available at ScienceDirect

Talanta

journal homepage: www.elsevier.com/locate/talanta

Short communication

Glucose biosensor based on immobilization of glucose oxidase in platinum nanoparticles/graphene/chitosan nanocomposite film

Hong Wu[a], Jun Wang[a], Xinhuang Kang[a], Chongmin Wang[a], Donghai Wang[a], Jun Liu[a], Ilhan A. Aksay[b], Yuehe Lin[a,*]

[a] Pacific Northwest National Laboratory, Richland, WA 99352, USA
[b] Department of Chemical Engineering, Princeton University, Princeton, NJ 08544, USA

ARTICLE INFO

Article history:
Received 1 May 2009
Received in revised form 17 June 2009
Accepted 17 June 2009
Available online 2 July 2009

Keywords:
Graphene
Platinum nanoparticles
Nanocomposite
Biosensor
Glucose

ABSTRACT

The bionanocomposite film consisting of glucose oxidase/Pt/functional graphene sheets/chitosan (GOD/Pt/FGS/chitosan) for glucose sensing is described. With the electrocatalytic synergy of FGS and Pt nanoparticles to hydrogen peroxide, a sensitive biosensor with a detection limit of 0.6 μM glucose was achieved. The biosensor also has good reproducibility, long-term stability and negligible interfering signals from ascorbic acid and uric acid comparing with the response to glucose. The large surface area and good electrical conductivity of graphene suggests that graphene is a potential candidate as a sensor material. The hybrid nanocomposite glucose sensor provides new opportunity for clinical diagnosis and point-of-care applications.

1. Introduction

Graphene has recently emerged as an interesting material in a myriad of applications because of its unique mechanical and electronic properties [1–5]. Most of the graphene studies have focused on its physical properties, such as its electronic properties, and these studies have demonstrated some applications in gas sensors [6,7] and pH sensors [8]. However, using graphene for biosensors has not received much attention. Graphene exhibits excellent electrical conductivity, high surface area, and strong mechanical strength [2,4,9]. Such properties indicate that graphene may be a good support for electrocatalysts. Recently, we developed a new approach for producing functionalized graphene sheets (FGSs) in mass quantities through the thermal expansion of graphite oxide to yield single graphene sheets with epoxy, hydroxyl, and carboxyl groups as well as Stone-Wales and 5–8–5 lattice defects [10]. Such functional groups and their lattice defects may play a significant role in preparing graphene-based electrocatalysts. Furthermore, these FGSs are more dispersible and biocompatible than other carbon-based materials due to their functional groups. These advantages of FGSs make them an ideal material for sensor and fuel cell applications. In fact, due to their planar morphology and thus larger accessible surface area, FGSs may perform better than any other carbon-based electrode as a sensor material. Another advantage of graphene is its potential low manufacturing cost as compared to other nanostructured carbon materials, such as carbon nanotubes. Recently, graphene has been used as electrode material for direct electrochemistry of glucose oxidase, battery, and fuel cell [11–13].

Noble nanoparticles (NPs), such as platinum, exhibit electrocatalytic behavior to hydrogen peroxide (H_2O_2) and have been widely used for sensing applications [14–16]. It will be attractive to prepare nanoparticle-functionalized FGS, e.g., platinum nanoparticles (Pt NP)/FGS nanocomposite, because such a functionalized FGS may generate synergy on electrocatalytic activity and thus enhance the sensitivity of the biosensor.

In this work, we report a FGS-based bionanocomposite film and demonstrate its application for sensitive glucose sensing. This bionanocomposite film was prepared by the following routes: chemically controlled modification of FGSs by electrodeposition of Pt NPs followed by physical modification of the Pt/FGS nanocomposite with enzymes. The FGS used here was prepared as described elsewhere [10]. The FGSs were first dispersed in a solution containing 0.2% chitosan and then cast on a glassy-carbon electrode (GCE). By using the potentiostatic electrodeposition in a platinum-containing solution, platinum nanoparticles were modified on the FGS/chitosan/GCE. Then glucose oxidase (GOD) was immobilized on Pt/FGS/chitosan/GCE, forming a bionanocomposite film.

* Corresponding author at: Pacific Northwest National Laboratory, 902 Battelle Blvd., PO Box 999, Richland, WA 99352, USA. Tel.: +1 509 376 0529; fax: +1 509 376 5106.
E-mail address: yuehe.lin@pnl.gov (Y. Lin).

0039-9140/$ – see front matter © 2009 Published by Elsevier B.V.
doi:10.1016/j.talanta.2009.06.054

2. Experimental

2.1. Chemicals

GOD, D-glucose, chitosan, phosphate buffer saline, potassium chloride, acetic acid, chloroplatinic acid, sulfuric acid, H_2O_2, ascorbic acid, and uric acid were all purchased from Sigma–Aldrich (St. Louis, USA). All solutions used in the experiments were prepared with ultra-pure water (18.3 MΩ cm, Nanopure, Barnstead, USA).

2.2. Materials

The graphene used in our study was made by thermal exfoliation of graphite oxide [10], which starts with the chemical oxidation of graphite flakes to increase the *c*-axis spacing from 0.34 nm to 0.7 nm. The resulting graphite oxide is split apart through rapid thermal expansion to yield a single but wrinkled graphene sheet functionalized with hydroxyl and epoxy sites.

2.3. Preparation of FGS/chitosan/GCE

The suspension of FGS was prepared by dispersing 1 mg graphene in 1 mL of 0.2% chitosan solution (pH 5). The mixture was sonicated 1 h to obtain a homogeneous dispersion. The FGS suspension was cast on the surface of a GCE (∅ = 3 mm) to prepare the FGS-modified electrode. Six microliters of 1 mg/mL FGS suspension was cast on the pretreated GCE and dried at room temperature.

2.4. Preparation of Pt/FGS/chitosan/GCE

Platinum nanoparticles were electrochemically deposited on the FGS/chitosan/GCE with constant potential at −0.25 V for a desired time in a 5-mL solution containing 1 mM H_2PtCl_4 and 0.5 M H_2SO_4. After the deposition, the electrode was thoroughly rinsed with water and allowed to dry at room temperature for further modification.

2.5. Preparation of GOD/Pt/FGS/chitosan/GCE

GOD was dissolved in a 0.2% chitosan solution, and the GOD concentration was 10 mg/mL. Six microliters of the solution were cast on the as-prepared Pt NP/FGS/chitosan/GCE. Right after casting, the GOD-modified electrode was moved into a refrigerator and kept at 4 °C to dry overnight. During the experimental period, the modified electrodes were stored at 4 °C until use.

2.6. Instrumentation

Cyclic voltammetric and amperometic measurements were performed on a CHI 824 electrochemical workstation (CHI Instruments, Inc., Austin, TX) connected to a personal computer. A three-electrode cell (10 mL) was employed with a modified GCE as the working electrode, an Ag/AgCl electrode as the reference electrode, and platinum wire as the auxiliary electrode. An amperometric response of the GOD/Pt/FGS/chitosan/GCE to the sequential addition of a desired amount of glucose was measured at +0.4 V with continuous gentle stirring in a 5-mL buffer solution containing 0.01 M PBS. The transmission electron microscope (TEM) images were recorded on a JEOL JEM 2010 microscope with a specified point-to-point resolution of 0.194 nm. The operating voltage on the microscope was 200 keV. The FGS sample was prepared by dropping a diluted FGS suspension onto the Cu–C grid. The Pt/FGS/chitosan nanocomposite sample was prepared by peeling the hybrid Pt/FGS/chitosan nanocomposite off the GCE and was transferred to a Cu–C grid. All images were digitally recorded with a slow-scan charge-coupled device camera (image size 1024 × 1024 pixels), and image processing was carried out using a Digital Micrograph (Gatan).

3. Results and discussion

The chitosan dispersed FGSs were prepared and characterized with TEM. Fig. 1(A) shows an image of FGSs dispersed in chitosan. As shown in this figure, the FGSs exhibit wrinkled graphene sheets. This wrinkled nature of FGSs is highly beneficial in maintaining a high surface area on the electrode since the sheets cannot readily collapse back to a graphitic structure. The inset in Fig. 1(A) displays a selected-area electron diffraction (SAED) of the nanocomposite material, yielding a double six-spot-ring pattern from a graphene sheet [17].

Pt nanoparticles were electrochemically deposited on FGS/chitosan film. Fig. 1(B) is a TEM image of Pt NP-modified FGSs. It can be seen from this figure that Pt NPs are uniformly deposited on the graphene surface with a size of less than 50 nm.

In the current study, the electrochemical response of the graphene-based glucose biosensor was coming from the anodic oxidation current of the enzymatic product H_2O_2. It is well known that H_2O_2 undergoes electrochemical oxidation processes at the solid electrodes, but the oxidation or reduction occur at relatively high potentials that cause high background current and interference from other electroactive compounds. Noble nanoparticles, such as platinum, have been widely used as electrocatalysts for oxidation and reduction of H_2O_2. To study the electrocatalytic effect of the FGS/chitosan and Pt/FGS/chitosan films to H_2O_2, cyclic

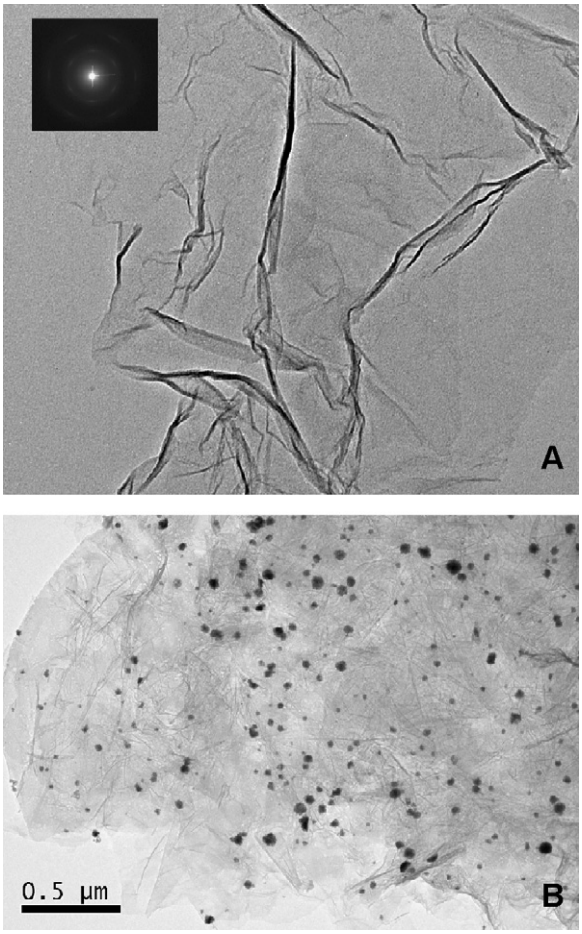

Fig. 1. (A) TEM image of FGS (inset: SAED of FGS). (B) TEM image of platinum nanoparticles deposited on a graphene sheet.

voltammetry was performed. Fig. 2(A) shows the cyclic voltammograms obtained at the modified GCE with a hybrid Pt/FGS/chitosan nanocomposite film in a 10-mM phosphate-buffered saline (PBS) solution containing 1.5 mM H_2O_2 in comparison with a bared GCE and FGS/chitosan GCE. The electrochemical responses of all these electrodes are negligible in the solution in the absence of H_2O_2 (data not shown). As shown in this figure, the oxidation and reduction currents from H_2O_2 at the bare GCE are quite small, and the oxidation of H_2O_2 at the bare GCE starts at 0.6 V. However, the electrochemical responses obtained at the FGS/chitosan/GCE and the Pt/FGS/chitosan/GCE are much larger than that obtained at the GCE. Moreover, it can be seen that the oxidation of H_2O_2 started at ~0.3 V, and the oxidation current increased as the potential increased at these modified electrodes. It can also be seen that the reduction of H_2O_2 started at 0.1 V at the modified electrode, and the reduction current increased as the potential decreased. The decrease of the overpotential of H_2O_2 is ascribed to the electrocatalytic activity of the platinum NP and graphene. Furthermore, it can be seen that the magnitude of the electrochemical response at these different electrodes increased in the following order: Pt/FGS/chitosan/GC > FGS/chitosan/GC > GC. It was concluded that the hybrid nanocomposite film with both graphene and platinum nanoparticles showed a synergistic effect on the electrocatalytic activity to H_2O_2. Therefore, the hybrid Pt/FGS/chitosan/GCE exhibited the highest electrocatalytic activity toward H_2O_2. The data from hydrodynamic voltammograms shown in Fig. 2(B) further confirmed the results in Fig. 2(A). Fig. 2(B) illustrates that the FGS-modified electrode improved the electrocatalytic activity to H_2O_2 (Curve b) compared with that at the GCE (Curve a). It can be seen that the Pt/FGS/chitosan nanocomposite had the highest electrochemical response to H_2O_2 and showed a significant synergistic effect on the electrocatalytic activity to H_2O_2 (Curve c).

The effect of the Pt electrodeposition time on the electrocatalytic activity of Pt/FGS/chitosan/GCE to H_2O_2 was studied. The electrocatalytic activity of the prepared electrode was measured at 0 V in a solution containing 0.6 mM H_2O_2. It was found that the response current increased as the deposition time increased until it reached the plateau at 200-s deposition. Then the signal started to decrease with more deposition time, which may be ascribed to the reduced electrochemical active surface area because large-sized particles may be deposited on the electrode surface with a long deposition time. A 200 s deposition time was chosen for this work.

Amperometric technique was used for the evaluation of the graphene-based biosensor for glucose detection. Fig. 3(A) shows the typical amperometric response of GOD/Pt/FGS/chitosan/GCE to successive additions of 0.15 mM glucose with an applied potential at 0.4 V. As can be seen from Fig. 3(A), the electrochemical response increased as the glucose concentration increased. From the inset in Fig. 3(A), it can be seen that the sensor is responsive to a low

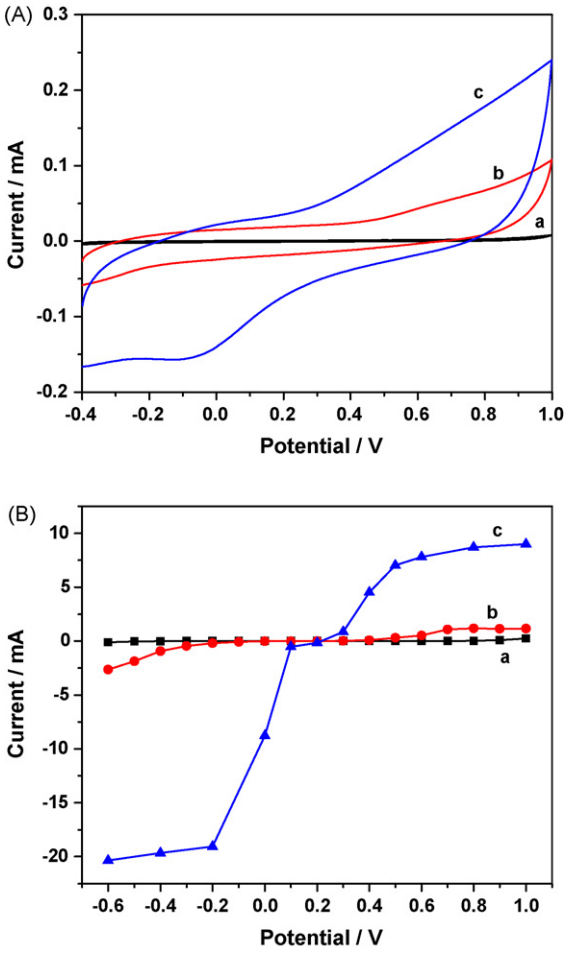

Fig. 2. (A) Cyclic voltammograms obtained at (a) bare GCE; (b) FGS/chitosan/GCE; (c) Pt/FGS/chitosan/GCE in 10 mM PBS buffer solution containing 1.5 mM H_2O_2. (B) Hydrodynamic voltammograms obtained at (a) bare GCE; (b) FGS/chitosan/GCE; (c) Pt/FGS/chitosan/GCE in 10 mM PBS buffer solution containing 0.12 mM H_2O_2.

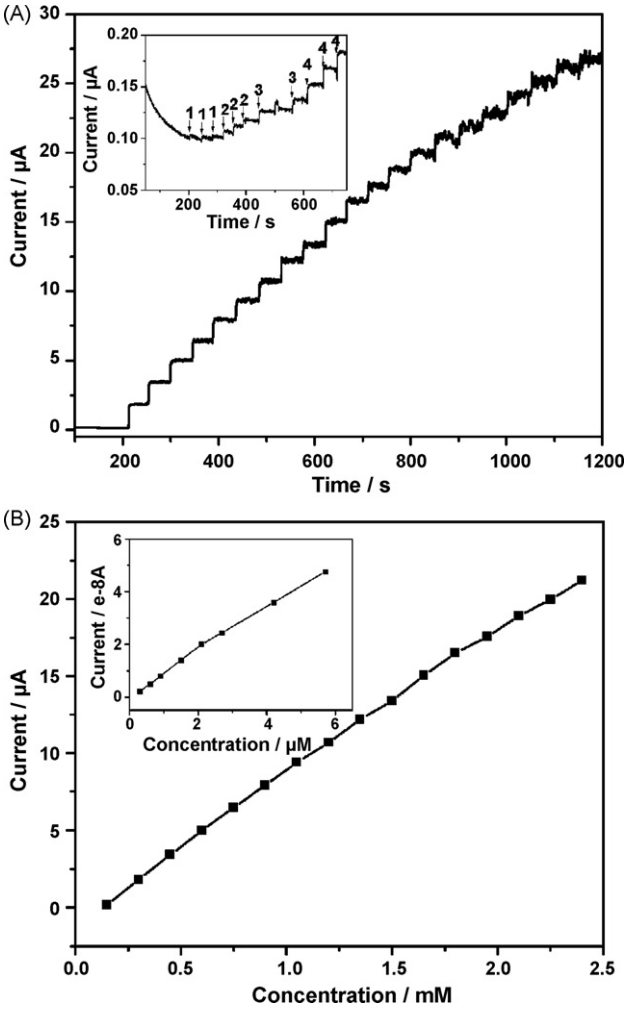

Fig. 3. (A) Amperometric response of GOD/Pt/FGS/chitosan/GCE to sequential addition of a series of glucose concentrations from 0.15 mM to 4.2 mM at +0.4 V. Inset (a) amperometric response to the sequential addition of (1) 0.3 μM, (2) 0.6 μM, (3) 1.5 μM, and (4) 3 μM glucose. (B) The calibration curve from (A). Inset (b) is the lower range of the calibration curve.

concentration of glucose, such as 0.6 μM glucose. Fig. 3(B) displays the plot of the electrochemical response vs. the glucose concentration. It can be seen from this figure that this sensor shows a wide linear range from sub-μM to 5 mM glucose. The detection limit of the glucose sensor is 0.6 μM based on the three times of signal-to-noise ratio. Such a sensitivity of the biosensor might be attributed to a large surface area, a fast electron transfer activity of FGS, and the electrocatalytic synergy from platinum and graphene. Within the nanocomposite, GOD can contact both graphene and platinum, which facilitates the fast electron transfer with a relatively low barrier between the enzyme and the electrode. The glucose sensor based on Pt NP/FGSs achieved a better detection limit in comparison with the Pt/Pb alloy NP/carbon nanotube-based glucose sensor [16] (a detection limit of 7 μM) and the Pt nanowire/carbon nanotube-based glucose sensor [15] (a detection limit of 3 μM). The sensitive biosensor was also accompanied with good reproducibility. The relative standard deviation (RSD) of the biosensor in response to 15 μM glucose was 6% for five different electrodes, indicating the good reproducibility of the biosensor. The long-term stability of the glucose sensor was examined with two electrodes for 2 weeks. The data showed that the enzyme maintained 86% of its activity during the first week and 75% during the second week. We also evaluated the potential interference from other electroactive biomolecules, such as ascorbic acid and uric acid, with concentrations similar to physiological fluid. Results indicate that the responses from these interferents are negligible. The sensor was also validated with glucose-spiked human plasma samples, and the recovery of the spike sample was 101%. These results indicate that the biosensor developed in this work has high sensitivity and selectivity for detecting blood glucose level.

4. Conclusion

We present a novel bionanocomposite film consisting of GOD/Pt/FGS/chitosan for glucose sensing. The biosensor exhibits good sensitivity with a detection limit of 0.6 μM glucose. Such a sensitivity is attributed to the synergy of FGS and Pt nanoparticles on the electrocatalytic activity to H_2O_2. The glucose biosensor has good responses because of the large surface area and fast electron transfer of graphene and Pt nanoparticles. The biosensor also has good reproducibility and long-term stability. The interfering signals from ascorbic acid and uric acid are negligible compared with the response to glucose. Human plasma samples were tested with the glucose sensor, and good recovery was achieved with the spiked samples. This work shows that the hybrid GOD/Pt/FGS/chitosan nanocomposite-based biosensor has great potential for clinical utility and home care for a rapid monitoring of glucose. The graphene-based biosensor fabrication method demonstrated in this work is readily applicable to the fabrication of other biosensors based on oxidases, such as biosensors for cholesterol, alcohol, lactate, acetylcholine, hypoxanthine, and xanthine [18,19].

Acknowledgements

This work was supported by a laboratory-directed research and development program at Pacific Northwest National Laboratory (PNNL). The work was performed at the Environmental Molecular Sciences Laboratory, a national scientific user facility sponsored by the U.S. Department of Energy (DOE) and located at PNNL. PNNL is operated by Battelle for DOE under Contract DE-AC05-76RL01830. Ilhan A. Aksay acknowledges support from Army Research Office (ARO)/Multidisciplinary Research Initiative (MURI) under grant number W911NF-04-1-0170 and the Directed Technologies, Inc.

References

[1] A.K. Geim, K.S. Novoselov, Nat. Mater. 6 (2007) 183.
[2] M. Wilson, Phys. Today 59 (2006) 21.
[3] C. Stampfer, E. Schurtenberger, F. Molitor, J. Guttinger, T. Ihn, K. Ensslin, Nano Lett. 8 (2008) 2378.
[4] D. Li, R.B. Kaner, Science 320 (2008) 1170.
[5] N.M.R. Peres, F. Guinea, A.H. Castro Neto, Phys. Rev. B 73 (2006) 125411.
[6] O. Leenaerts, B. Partoens, F.M. Peeters, Phys. Rev. B 77 (1–6) (2008) 125416.
[7] B. Huang, Z. Li, Z. Liu, G. Zhou, S. Hao, J. Wu, B. Gu, W.H. Duan, J. Phys. Chem. C 112 (2008) 13442.
[8] P.K. Ang, W. Chen, A.T.S. Wee, K.P. Loh, J. Am. Chem. Soc. 130 (2008) 14392.
[9] R.M. Westervelt, Science 320 (2008) 324.
[10] (a) H.C. Schniepp, J.-L. Li, M.J. McAllister, H. Sai, M. Herrera-Alonso, D.H. Adamson, R.K. Prud'homme, R. Car, D.A. Saville, I.A. Aksay, J. Phys. Chem. B 110 (2006) 8535;
(b) M.J. McAllister, J.-L. Li, D.H. Adamson, H.C. Schniepp, A.A. Abdala, J. Liu, M. Herrera-Alonso, D.L. Milius, R. Car, R.K. Prud'homme, I.A. Aksay, Chem. Mater. 19 (2007) 4396.
[11] C. Shan, H. Yang, J. Song, D. Han, A. Ivaska, L. Niu, Anal. Chem. 81 (2009) 2378.
[12] D. Wang, D. Choi, J. Li, Z. Yang, Z. Nie, R. Kou, D. Hu, C. Wang, L.V. Saraf, J. Zhang, I.A. Aksay, J. Liu, ACS Nano 3 (2009) 907.
[13] R. Kou, Y. Shao, D. Wang, M.H. Engelhard, J.H. Kwak, J. Wang, V. Viswanathan, C. Wang, Y. Lin, Y. Wang, I.A. Aksay, J. Liu, Electrochem. Commun. 11 (2009) 954.
[14] X. Chu, D. Duan, G. Shen, R. Yu, Talanta 71 (2007) 2040.
[15] F. Qu, M. Yang, G. Shen, R. Yu, Biosens. Bioelectron. 22 (2007) 1749.
[16] H. Cui, J. Ye, W. Zhang, C. Li, J.H.T. Luong, F. Sheu, Anal. Chim. Acta 594 (2007) 175.
[17] K.S. Novoselov, A.K. Geim, S.V. Morozov, D. Jiang, Y. Zhang, S.V. Dubonos, I.V. Grigorieva, A.A. Firsov, Science 306 (2004) 666.
[18] J. Wang, Y. Lin, Trends Anal. Chem. TrAC 27 (2008) 619.
[19] M. Jiang, Y. Lin, in: C.A. Grimes, E.C. Dickey, M.V. Pishko (Eds.), Encyclopedia of Sensors, vol. 2, American Scientific Publishers, Stevenson Ranch, CA, 2006, pp. 25–51.